BIODIVERSITY RESEARCH

An integrated, spatio-temporal modelling framework for analysing biological invasions

Thomas Mang[1,2] (iD) | Franz Essl[2,3,4] | Dietmar Moser[1,2] | Ingrid Kleinbauer[1] | Stefan Dullinger[2]

[1]Vienna Institute for Nature Conservation & Analyses, Vienna, Austria

[2]Division of Conservation Biology, Vegetation Ecology and Landscape Ecology, Department of Botany and Biodiversity Research, University of Vienna, Vienna, Austria

[3]Environment Agency Austria, Vienna, Austria

[4]Centre of Excellence for Invasion Biology, Stellenbosch University, Stellenbosch, South Africa

Correspondence
Thomas Mang, Division of Conservation Biology, Vegetation Ecology and Landscape Ecology, Department of Botany and Biodiversity Research, University of Vienna, Vienna, Austria.
Email: thomas_mang@univie.ac.at

Funding information
Austrian Academy of Sciences, Grant/Award Number: 22636; Klima- und Energiefonds, Grant/Award Number: B068662

Editor: José Lahoz-Monfort

Abstract

Aim: We develop a novel modelling framework for analysing the spatio-temporal spread of biological invasions. The framework integrates different invasion drivers and disentangles their roles in determining observed invasion patterns by fitting models to historical distribution data. As a case study application, we analyse the spread of common ragweed (*Ambrosia artemisiifolia*).

Location: Central Europe.

Methods: A lattice system represents actual landscapes with environmental heterogeneity. Modelling covers the spatio-temporal invasion sequence in this grid and integrates the effects of environmental conditions on local invasion suitability, the role of invaded cells and spatially implicit "background" introductions as propagule sources, within-cell invasion level bulk-up and multiple dispersal means. A modular framework design facilitates flexible numerical representation of the modelled invasion processes and customization of the model complexity. We used the framework to build and contrast increasingly complex models, and fitted them using a Bayesian inference approach with parameters estimated by Markov chain Monte Carlo (MCMC).

Results: All modelled invasion drivers codetermined the *A. artemisiifolia* invasion pattern. Inferences about individual drivers depended on which processes were modelled concurrently, and hence changed both quantitatively and qualitatively between models. Among others, the roles of environmental variables were assessed substantially differently subject to whether models included explicit source-recipient cell relationships, spatio-temporal variability in source cell strength and human-mediated dispersal means. The largest fit improvements were found by integrating filtering effects of the environment and spatio-temporal availability of propagule sources.

Main conclusions: Our modelling framework provides a straightforward means to build integrated invasion models and address hypotheses about the roles and mutual relationships of different putative invasion drivers. Its statistical nature and generic design make it suitable for studying many observed invasions. For efficient invasion modelling, it is important to represent changes in spatio-temporal propagule supply by explicitly tracking the species' colonization sequence and establishment of new populations.

1 | INTRODUCTION

Invasive alien species (IAS) represent an important component of global environmental change (Pyšek & Richardson, 2010; Vitousek, D'Antonio, Loope, & Westbrooks, 1996) and may threaten native biodiversity (Bellard, Cassey, & Blackburn, 2016; Mack et al., 2000), cause economic damage (Pejchar & Mooney, 2009; Pimentel, Zuniga, & Morrison, 2005) and affect health (Medlock et al., 2012; Taramarcaz, Lambelet, Clot, Keimer, & Hauser, 2005). From a scientific perspective, biological invasions also provide unique opportunities for real-time investigations of ecological processes and their underlying spatial and temporal dynamics at multiple scales (Pauchard & Shea, 2006; Sakai et al., 2001; Strayer, Eviner, Jeschke, & Pace, 2006). Moreover, a sound understanding of invasion processes is a precondition for successfully managing the spread of potentially detrimental species.

A central approach to investigating the drivers of biological invasions involves modelling the spatio-temporal spread pattern. The development and application of such spread models has been an active field of interplay between theoretical and empirical works for decades (Hastings et al., 2005). Commonly applied modelling approaches include the following: ecological niche models (species distribution models) which assess spatial variation in invasion susceptibility by correlating alien species occurrences with prevailing environmental conditions (Elith, Kearney, & Phillips, 2010; Peterson, 2003; Petitpierre et al., 2012); spread rate models, such as integrodifference equations which describe local population development for various forms of population structuring and spatial redistribution probabilities of propagules (Jongejans, Shea, Skarpaas, Kelly, & Ellner, 2011; Kot, Lewis, & van den Driessche, 1996; Neubert & Parker, 2004); and models of long-distance, human-mediated spread along selective dispersal corridors such as traffic routes (Drake & Mandrak, 2010; Muirhead et al., 2006; Potapov, Muirhead, Lelea, & Lewis, 2011).

Each of these modelling approaches focuses on different invasion drivers. However, for many invasions, the various drivers jointly determine the spread. With advances in computational techniques, modelling multiple invasion drivers becomes increasingly feasible. Among such models, simulation models have been used to investigate the large-scale spread pattern in a bottom-up manner by simulating the development and interactions of many small entities, typically individuals or populations (Andrew & Ustin, 2010; Fitzpatrick, Preisser, Porter, Elkinton, & Ellison, 2012; Merow, LaFleur, Silander, Wilson, & Rubega, 2011; Sebert-Cuvillier et al., 2010). However, a central prerequisite of this approach is that the relevant drivers and the demographic responses to them are well known and can be sufficiently accurately parameterized. By contrast, statistical approaches fit models and estimate parameters based on historical spread data (Kadoya & Washitani, 2010; Marion et al., 2012; Smolik et al., 2010; Wikle,

2003). However, the roles of the different processes and drivers that determine the historical spread patterns often remain poorly understood. For example, at larger geographical scales, observed spatio-temporal invasion patterns are usually assumed to be driven by a combination of environmental niche constraints, randomly placed introductions, propagule production and available dispersal means (Pyšek & Richardson, 2007), but the relative impacts of these processes are seldom disentangled.

In this study, we develop and demonstrate a novel framework for analysing biological invasions. This framework jointly models the effects of different drivers on the spatio-temporal spread of alien species and allows for addressing specific hypotheses about their relevance and contribution to generating observed invasion patterns. We illustrate the framework with a case study analysis of the common ragweed (*Ambrosia artemisiifolia* L., Asteraceae) invasion in Central Europe. By building and contrasting increasingly complex models, we show how the integrated modelling approach improves our understanding of the impacts of and the mutual dependencies between (hypothesized) main invasion drivers.

2 | METHODS

2.1 | Framework outline

In our framework, the study area is represented by a lattice system of discrete cells (Figure 1a). The framework traces the invasion sequence in this grid by modelling the time of first invasion in each grid cell (Cook, Marion, Butler, & Gibson, 2007). To describe local environmental suitability for the invading species (Elith et al., 2010), grid cells are assigned environmental attributes such as climatic conditions, availability of particular habitat types or characteristics of recipient communities. Attributes can change over time. Cells uninvaded at a given time are potential recipient cells exposed to an invasion risk. This risk is quantified as a combined measure of the imposed propagule pressure and the local environmental suitability for the invading species. Cells already invaded at a given time act as propagule sources. The propagule production rate in source cells depends on the local environmental suitability of these cells and within-cell invasion level dynamics (Pagel & Schurr, 2012). The dispersal rate from source to recipient cells is quantified using measures of the spatial relationship between cells such as geographical distance (Kot et al., 1996) or connectivity along selective dispersal corridors (Drake & Mandrak, 2010). The magnitude of the propagule pressure exerted by a source cell on a recipient cell is proportional to the propagule production rate in the source cell and the dispersal rate from source to recipient cell. We further use "background" introductions to represent
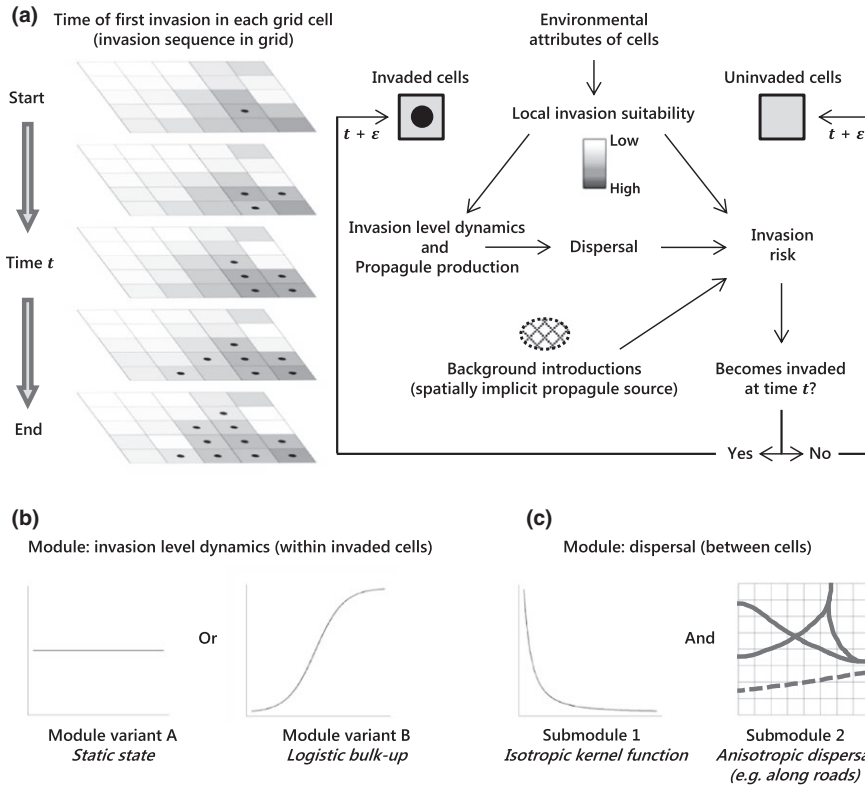
(a)

FIGURE 1 Schematic illustration of the invasion modelling framework. (a) A two-dimensional lattice system represents the study area, including environmental variability over time. The framework models the time of first invasion in each grid cell dependent on a number of ecological processes, each implemented as a separate framework module. (b) For individual modules, exchangeable definitions can be provided, as illustrated here by the invasion level dynamics within a source cell represented either by a static state or logistic bulk-up. (c) Framework modules may themselves be expressed as a collection of submodules, such as net dispersal which is formed by summing up multiple independent dispersal means

a global, spatially implicit propagule source (for example, to represent introductions from outside the study area, including the species' native range) and which hence expose recipient cells to propagule pressure independent of already invaded cells. It is assumed that the species persists in a cell once invaded (Figure 1a).

The invasion risk imposed on recipient cell i at time t, $g_i(t)$, is quantified by the invasion risk function which integrates the above processes using the general form

$$g_i(t) \propto \left[\sum_{j \in \Omega(t)} P_j(t) D_{j,i}(t) + U_i(t) \right] S_i(t), \tag{1}$$

where $\Omega(t)$ is the set of cells invaded at time t, $P_j(t)$ is the propagule production rate of source cell j and $D_{j,i}(t)$ is the dispersal rate from this source cell to the recipient cell at time t, $U_i(t)$ is the background introduction rate imposed on the recipient cell at time t, and $S_i(t)$ is the local environmental suitability of the recipient cell at time t. The environmental attributes of cells i and j are used in the specifications of $S_i(t)$ and $P_j(t)$, respectively. In numerical terms, equation (1) represents the rate at which uninvaded cells are exposed to invasion, and uses continuous time. This rate defines the probability distribution of cell invasion time, that is the time of first invasion into a recipient cell, as follows (for details and an extended discussion, see Appendix S1 in Supporting Information): let a grid cell be uninvaded at the model start time t_s, expose it to invasion risk as quantified by $g(t)$ and let X be the random variable of cell invasion time; then, the probability that the cell remains uninvaded until time x is given by the so-called survival function

$$S_X(x; g(t), t_s) = P(X > x; g(t), t_s) = e^{-\int_{t_s}^{x} g(t)dt} \tag{2}$$

(for $x \geq t_s$). Evaluated for the model end time, t_e, that is $x = t_e$, the survival function hence states the probability that the cell remains uninvaded during the modelling period.

Dates of distribution data typically refer to discrete time units (e.g. years). Let t_{s_k} and t_{e_k} denote the start and end time of the k-th discrete modelling subperiod (e.g. a given year), respectively; then, the probability that cell invasion occurs in the k-th subperiod is given by the probability mass function

$$f_X(x_k; g(t), t_s) = P(X = x_k) = e^{-\int_{t_s}^{t_{s_k}} g(t)dt} - e^{-\int_{t_s}^{t_{e_k}} g(t)dt}. \tag{3}$$

Higher values of $g(t)$ correspond to earlier expected invasion time.

In the framework's statistical set-up, the likelihood function considers each grid cell's invasion time (Cook et al., 2007). Let $\boldsymbol{x}$ be the invasion times of all grid cells, $\boldsymbol{\theta}$ be all parameters which codetermine invasion risk, $\boldsymbol{\Psi}_m$ be the set of cells which are invaded during the modelling period and $\boldsymbol{\Psi}_e$ be the set of cells which remain uninvaded until the model end time, then the likelihood function is

$$\mathcal{L}(\boldsymbol{\theta}|\boldsymbol{x}) = \prod_{i \in \Psi_m} f_{X_i}(x_i; g_i(t), t_s) \times \prod_{i \in \Psi_e} S_{X_i}(t_e; g_i(t), t_s) \tag{4}$$

(for further information, see Appendix S1).

To implement the framework for a given invasion analysis, the processes embedded in equation (1) must be numerically defined. We propose a modular approach in which each process is captured by a separate framework module, thus establishing

a traceable mapping between ecological process understanding and quantitative model implementation. This modular design brings several advantages: (i) each module can be specified independently; (ii) models can combine different modules, or test alternative representations of the same process by exchanging the numerical module implementation (Figure 1b); and (iii) by applying modularity recursively, main modules can be constructed from multiple lower-level modules (Figure 1c). Modularity thus facilitates the testing of alternative model representations or the customization of the framework to different invasion studies. Framework modules and parameters are scaled to species spread at the grid cell level and hence do not represent the actual ecological quantities from which they emerge (such as the number of propagules produced by an individual). We illustrate the modular approach with the invasion of *A. artemisiifolia* in Central Europe as a case study.

2.2 | *Ambrosia artemisiifolia* invasion in Central Europe

Native to central North America, *Ambrosia artemisiifolia* is an annual, wind-pollinated herb adapted to temperate climates. The first European records stem from the 19th century but spread and subsequent naturalization only started in the first decades of the 20th century (Essl et al., 2015; and references therein). Range expansion then gained momentum after World War II, and in particular since ca. 1990. Occurrences are mostly concentrated in warmer lowland areas, and temperature was shown to act as an important invasion filter (Chapman, Haynes, Beal, Essl, & Bullock, 2014). As germination and early seedling establishment require disturbed soil surfaces, the species is primarily found in agricultural fields, disturbed open habitats in and around human settlements, roadsides and railway tracks, and rarely invades closed vegetation. The trade of contaminated goods and vehicle traffic facilitate long-distance dispersal. Seeds are persistent in the soil seed bank for several decades and invaded sites hence remain occupied for a long time. The *A. artemisiifolia* invasion is of high public health concern as the species produces the most allergenic pollen of any plant species occurring in Europe, causing enormous costs (Essl et al., 2015).

2.2.1 | Study area and period

The study area in Central Europe includes Austria, the Czech Republic, Germany, Hungary, Liechtenstein, Slovakia, Slovenia and Switzerland, spanning a contingent area of over 700,000 km^2 (Figure 2). These countries cover a range of climates with lowland continental areas in the east, oceanic climate towards the north, and montane and alpine zones in the south and south–west. The study area was represented by a lattice system with 5′×3′ (~ 6 × 6 km^2) cells corresponding to the Central European Floristic Mapping Project, comprising 22,451 cells in total. We modelled the historical *A. artemisiifolia* invasion progress from 1900 to 2010 at an annual resolution.

2.2.2 | Distribution data

Species records (spatio-temporal occurrence data) were gathered from many different sources (e.g. floristic mapping projects, floristic publications, major herbaria, unpublished own records and of colleagues), mapped to a grid cell and the observation dates (years) extracted from the original source (see Appendix S2). A total of 11,800 records document 3,598 cells as invaded by 2010 (Figure 2; Table S1). Species records were condensed to time of first invasion in each of the cells (**x**) using the date of the earliest record from each cell. Although we aimed for as comprehensive a distribution dataset as possible, it is acknowledged that due to the large spatio-temporal study extent, some inaccuracy with respect to prompt and complete recording of new species occurrences remains inevitable.

2.3 | Case study modelling

2.3.1 | Module definitions

Our case study application used the following module definitions.

The dependence of a cell's relative invasion suitability on environmental conditions is given by

$$S_i(t) = f_s(\mathbf{v}_{i,t} \cdot \boldsymbol{\beta}) \frac{a_i}{\bar{a}}, \tag{5}$$

where the vector $\mathbf{v}_{i,t}$ represents the environmental attributes of cell i at time t and the vector $\boldsymbol{\beta}$ represents the associated weighting parameters (to be estimated by model fitting), f_s is a transformation function, a_i is the cell's terrestrial area, and $\bar{a}$ is the mean terrestrial area across all cells. We used $f_s(z) = \exp(z)$ (Cook et al., 2007; Faraway, 2006) to yield a gradual, relatively scaled suitability measure. Based on the ecology of *A. artemisiifolia*, the following six environmental variables were used: mean temperature and total precipitation of the growing season (April–October); the proportion of cropland area and of urban area; and the length (scaled relative to area) of motorways and railways to test whether these infrastructure networks also offered suitable disturbance habitats, aside from their role in promoting dispersal (DiTommaso, 2004; Dullinger, Kleinbauer, Peterseil, Smolik, & Essl, 2009; Essl et al., 2015). Non-climate variables were log-transformed to improve symmetry and reduce the impact of outlier values. All environmental variables were standardized (subtraction of sample mean and division by sample standard deviation), and the obtained parameter estimates hence represent relative effect sizes as larger parameter magnitudes correspond to greater impacts of the associated environmental variables on invasion suitability. For details of data sources and processing, see Appendix S3.

The invasion level of an individual source cell, and therefore also its source strength, is modelled to develop (spatially implicitly within the cell) according to the differential equation

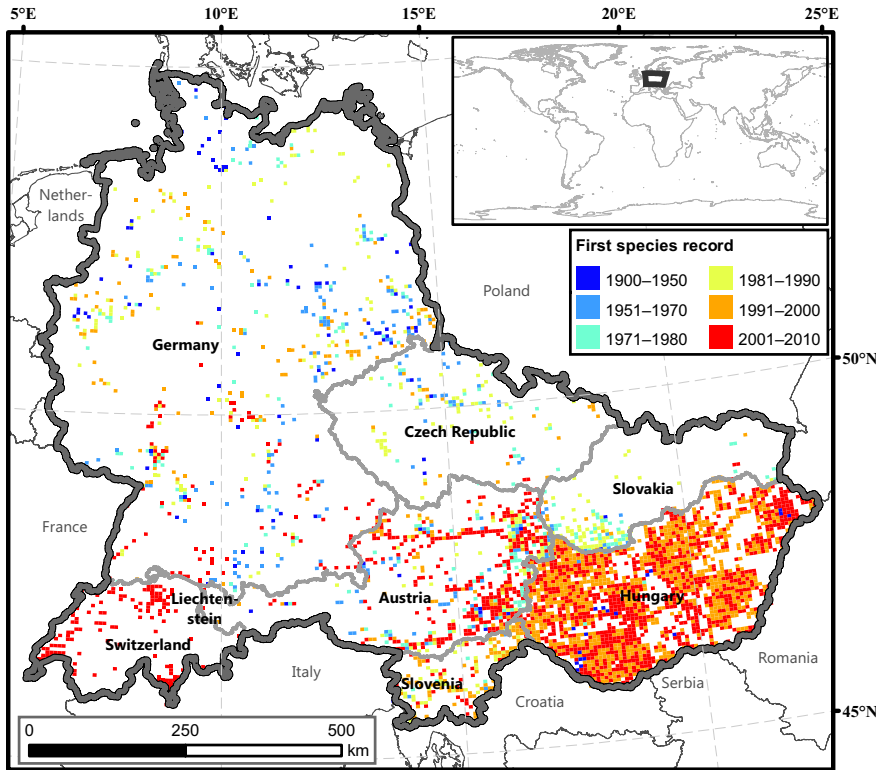$$\frac{dN_i}{dt} = (s + r N_i)\left(1 - \frac{N_i}{K_i}\right), \tag{6a}$$

FIGURE 2 *Ambrosia artemisiifolia* L. (Asteraceae) invasion history in Central Europe for the modelling period 1900–2010. Grid cell size is 5′×3′ (~ 6 × 6 km²). Map projection: Lambert azimuthal equal-area. [Colour figure can be viewed at wileyonlinelibrary.com]

which has the solution

$$N_i(t) = K_i - \frac{K_i \left(\frac{s}{K_i} + r \right)}{r + \left(\frac{s + rN_0}{K_i - N_0} \right) \left(e^{\left(\frac{s}{K_i} + r \right)(t - x_i)} \right)}.$$

(6b)

Here, $N_i(t)$ is the invasion level at time t, N_0 is the initial invasion level at the cell's invasion time x_i, r is an intrinsic and s an extrinsic growth rate, and K_i is the cell's maximum invasion level. Equation (6) is a variant of logistic growth (Tsoularis & Wallace, 2002) in which r controls bulk-up due to local reproduction, and s due to external propagule influx. For the annual species *A. artemisiifolia*, we used $K_i(t) = S_i(t)$, so the maximum invasion level is a relative measure of a cell's suitability for sustaining large populations based on local environmental conditions. Equation (6b) was evaluated stepwise (annual intervals) for piecewise-constant values of K_i, and $N_i(t)$ was constrained to be $K_i(t)$ at most (including the case of K_i dropping between successive years).

We model both isotropic dispersal (redistribution probabilities of propagules identical in all directions) and anisotropic dispersal (redistribution probabilities vary with direction). For isotropic dispersal, we started with a leptokurtic, one-dimensional kernel function from the power-law family of form $f_{1D}(d_{j,i}) = d_{j,i}^{-\alpha}$ (Portnoy & Willson, 1993), where $d_{j,i}$ is the Euclidean distance (in km) between the centroids of cells j and i, and α is a shape parameter. To match the lattice system dimensionality, this base function was then projected into two-dimensional space and normalized to yield the isotropic kernel function $f_{2D}(d_{j,i})$ (see Appendix S4). For anisotropic dispersal, we model selective, human-mediated propagule flow along infrastructure networks of (major) roads and railways. Net dispersal sums both dispersal means:

$$D_{j,i}(t) = f_{2D}(d_{j,i}) + \sum_{k \in \{rd,rw\}} \frac{b_{k,t}}{c_{k,j,i}} \omega_k,$$

(7)

where for anisotropic dispersal, rd and rw correspond to road and railway networks, respectively, $b_{k,t}$ is the flow intensity along network type k at time t due to traffic and trade, $c_{k,j,i}$ is the network type cost-distance (inversely related to connectivity) between cells j and i, and ω_k is a flow rate parameter (Drake & Mandrak, 2010). For details of data sources and processing, see Appendix S3.

Background introductions represent a global propagule source with no specified relationship to invaded cells. They include processes such as introduction via international trade of contaminated goods (Chapman et al., 2016). The background introduction rate is modelled using a time trend with linear and exponential terms:

$$U_i(t) = \left[\lambda_0 (\lambda_1 (t - t_s) + e^{\lambda_2 (t - t_s)}) + \lambda_b \mathbf{1}(t = t_s) \right] e^{w_i \tau},$$

(8)

where t_s is the model start time (1900), the parameter λ_0 defines the base rate, λ_1 and λ_2 control the time trend shape, and λ_b provides an additional boost applicable only to the model start time (via the indicator function $\mathbf{1}$). This boost represents all propagule pressure accumulated prior to the modelling period; for a further discussion of its general usefulness, see Appendix S1. Introduction rates are spatially modulated by w_i, the inverse of the squared cell distance to the nearest terrestrial border of the study area (log-transformed and standardized); this term reduces edge-effect biases by exposing grid cells near this border to elevated propagule pressure, whose magnitude is dependent on the parameter τ, to compensate for the lower average number of grid cells in their neighbourhood.

For the annual species *A. artemisiifolia*, the propagule production of source cells is assumed to be directly proportional to their invasion level. Moreover, since seed production occurs at the end of the growing season while the invasion times of cells refer to the first adult plant occurrence in recipient cells, for the invasion risk function used by our models an offset of one year applies:

$$g_i(t) = \left[\sum_{j \in \Omega(t-1)} \eta \, N_j(t-1) \, D_{j,i}(t-1) + U_i(t) \right] S_i(t), \qquad (9)$$

where the parameter η is the propagule production rate of source cells per unit invasion level. For species with different life-history traits, adjustments may be required.

2.3.2 | Model hierarchy

We constructed a model hierarchy which successively integrates an increasing number of invasion drivers, and tested the impact of these drivers on both module-wise and overall invasion inferences. The hierarchy was derived by combining different modules and/or replacing relevant free module parameters by cancel-out constants (cf. Table 1). Each model extends its predecessor; see Table 1 for a full list of parameters to estimate in each model.

The Null-model fits the invasion history using only the terrestrial area of grid cells and a temporally constant rate of background introductions as the sole propagule source; invaded cells do not propagate spread.

Model 1 uses all environmental variables to describe differences in the invasion suitability of cells. This set-up resembles a niche modelling approach as cell invasions are driven exclusively by environmental heterogeneity and without any dependencies between cells.

Model 2 introduces temporal variability in invasion rates using the time trend for background introductions.

Model 3 enables explicit source-recipient cell relationships by adding a generic propagule production rate to invaded cells and isotropic dispersal from invaded to uninvaded cells. The invasion risk imposed on recipient cells increases as progressively more cells become invaded, subject to the spatial proximity to these source cells.

Model 4 adds the edge-effects term to background introductions; this term was not incorporated into Model 3 so its impact can be clearly distinguished from that of explicit source-recipient cell relationships.

Model 5 introduces within-cell invasion level dynamics, and therefore also spatio-temporal variability in the propagule production of source cells.

Model 6 finally integrates anisotropic dispersal along roads and railways.

2.3.3 | Model fitting

All models were fitted to the observed invasion sequence of *A. artemisiifolia* in Central Europe using a Bayesian inference approach with Markov chain Monte Carlo (MCMC) for parameter estimation (Gelman, Carlin, Stern, & Rubin, 2004). The Bayesian approach infers the full posterior distribution of all model parameters, and MCMC is well suited for fitting models of higher parameter dimensionality. This

aligns well with the statistical nature and generic design of our framework. We used vague (marginal) prior distributions for all parameters (Table S2), and the posterior distributions were hence virtually exclusively determined by the data. For all models, 100,000 iterations were sampled after burn-in; for the most complex model, Model 6, this required about 57 hr of execution time on a workstation with an Intel® Core i7-3930K processor and an AMD Tahiti device using a parallel computing implementation developed in C++. For further MCMC details, see Appendix S5.

Parameter estimates were summarized by the (marginal) posterior distribution median and the 95% (central) credible interval. For parameters with a null-hypothesis value located in the interior of the corresponding distribution support, the Bayesian kind of significance testing assesses if the credible interval overlaps the null-hypothesis value. In our models, this applied to β and τ, with 0 as the null-hypothesis value for a neutral effect.

The importance of entire invasion processes was assessed by contrasting models for significant fit improvement using the Deviance Information Criterion (DIC) (Spiegelhalter, Best, Carlin, & van der Linde, 2002), the Bayesian analogue of the frequentist Akaike Information Criterion (AIC). The model with the lowest DIC is preferred and, roughly speaking, a DIC difference (ΔDIC) of 5–10 indicates a substantial difference, and a ΔDIC of >10 implies one model being definitely superior.

For quantifying model fit, we compared the annual invasion probabilities of cells (conditional on cells not having been invaded by the preceding year, and based on the mean of the sampled posterior distribution) with observed invasion outcomes by calculating (i) the area under the receiver operating characteristic (ROC) curve, AUC; and (ii) Tjur's coefficient of discrimination (Tjur, 2009), a pseudo-R^2 variant which calculates the difference between the means of the model-predicted probabilities for the outcome classes.

3 | RESULTS

3.1 | Parameter estimates

Among the variables used to characterize a cell's environmental suitability to *A. artemisiifolia* invasion, temperature, precipitation and the proportion of urban area per grid cell were significant in all six models (Table 1). Temperature was by far the most important predictor throughout (largest parameter magnitude), followed by precipitation. However, as model complexity increased, parameter estimates generally shrank, hence reducing the discriminative effect of the environment (see Appendix S6, Figure S1). Because of this, only in Model 1 were all environmental variables significant. Motorway length was significant in Models 1–4, and railway length in all but Model 6 which integrated anisotropic dispersal along infrastructure networks. This suggested that predominant dispersal effects may actually have been masked by apparent habitat effects in the less complex models. For all models, the credible intervals remained relatively compact and homogeneously sized. Therefore, within a given model, the impact of each environmental variable was estimated with low uncertainty. However,

TABLE 1 Parameter estimates for the models of *Ambrosia artemisiifolia* invasion in Central Europe. Estimates are stated as median (top row / before the semicolon) and 95% (central) credible interval (bottom row / after the semicolon) of the marginal posterior distributions. Significance tests are applicable only to τ and invasion suitability parameters, with significant results marked by *. Cancel-out constants replace parameter estimates if the respective parameters are not used by a given model.

Part 1: Null-model and Models 1–3					
Parameter	**Cancel-out constant**	**Null-model**	**Model 1**	**Model 2**	**Model 3**
Background introductions					
Start time boost, λ_b	0	5.55×10^{-5}; $(4.84 \times 10^{-6}, 2.22 \times 10^{-4})$	3.02×10^{-5}; $(2.92 \times 10^{-6}, 1.17 \times 10^{-4})$	8.21×10^{-5}; $(1.70 \times 10^{-5}, 2.20 \times 10^{-4})$	1.13×10^{-4}; $(2.51 \times 10^{-5}, 3.00 \times 10^{-4})$
Base rate, λ_0	0	1.48×10^{-3}; $(1.43 \times 10^{-3}, 1.53 \times 10^{-3})$	4.78×10^{-4}; $(4.49 \times 10^{-4}, 5.09 \times 10^{-4})$	1.04×10^{-5}; $(8.04 \times 10^{-6}, 1.29 \times 10^{-5})$	1.06×10^{-5}; $(5.82 \times 10^{-6}, 1.66 \times 10^{-5})$
Time trend - linear, λ_1	0			1.22×10^{-2}; $(1.07 \times 10^{-3}, 5.42 \times 10^{-2})$	1.40×10^{-2}; $(1.18 \times 10^{-3}, 8.06 \times 10^{-2})$
Time trend - exponential, λ_2	0			5.13×10^{-2}; $(4.91 \times 10^{-2}, 5.38 \times 10^{-2})$	3.58×10^{-2}; $(3.07 \times 10^{-2}, 4.17 \times 10^{-2})$
Edge-effects, τ	0				
Invasion suitability (due to environment)					
$\beta_{temperature}$	0		1.91; (1.86, 1.96)*	1.70; (1.65, 1.76)*	1.14; (1.08, 1.20)*
$\beta_{precipitation}$	0		0.58; (0.54, 0.62)*	0.45; (0.41, 0.49)*	0.41; (0.37, 0.45)*
$\beta_{cropland\ area}$	0		0.07; (0.01, 0.12)*	-0.01; (-0.07, 0.05)	-0.02; (-0.07, 0.04)
$\beta_{urban\ area}$	0		0.46; (0.42, 0.51)*	0.18; (0.14, 0.22)*	0.18; (0.13, 0.22)*
$\beta_{motorways}$	0		0.10; (0.07, 0.13)*	0.05; (0.02, 0.07)*	0.03; (0.00, 0.06)*
$\beta_{railways}$	0		0.04; (0.00, 0.08)*	0.14; (0.10, 0.18)*	0.13; (0.09, 0.17)*
Isotropic dispersal, α	$\to \infty$ (all $d_{j,i} \geq 1$)				1.19; (1.11, 1.27)
Source cells propagule production rate, η	0				2.94×10^{-2}; $(2.72 \times 10^{-2}, 3.17 \times 10^{-2})$
Invasion level dynamics (within-cell)					
Initial value, N_0	$N_0 = K_i = 1$				
Intrinsic growth rate, r	0				
Extrinsic growth rate, s	0				
Anisotropic dispersal (along networks)					
ω_{roads}	0				
$\omega_{railways}$	0				

Part 2: Models 4–6				
Parameter	**Cancel-out constant**	**Model 4**	**Model 5**	**Model 6**
Background introductions				
Start time boost, λ_b	0	9.83×10^{-5}; $(2.40 \times 10^{-5}, 2.58 \times 10^{-4})$	1.14×10^{-4}; $(2.45 \times 10^{-5}, 3.02 \times 10^{-4})$	1.14×10^{-4}; $(2.57 \times 10^{-5}, 3.01 \times 10^{-4})$
Base rate, λ_0	0	4.40×10^{-6}; $(1.35 \times 10^{-6}, 8.39 \times 10^{-6})$	1.27×10^{-5}; $(6.60 \times 10^{-6}, 2.05 \times 10^{-5})$	8.90×10^{-6}; $(3.83 \times 10^{-6}, 1.56 \times 10^{-5})$
Time trend - linear, λ_1	0	2.72×10^{-2}; $(2.06 \times 10^{-3}, 2.91 \times 10^{-1})$	1.36×10^{-2}; $(1.13 \times 10^{-3}, 8.10 \times 10^{-2})$	1.78×10^{-2}; $(1.38 \times 10^{-3}, 1.31 \times 10^{-1})$

(Continues)

TABLE 1 (Continued)

Parameter	Cancel-out constant	Model 4	Model 5	Model 6
Part 2: Models 4–6				
Time trend - exponential, λ_2	0	4.27×10^{-2}; $(3.61 \times 10^{-2}, 5.37 \times 10^{-2})$	3.52×10^{-2}; $(2.99 \times 10^{-2}, 4.12 \times 10^{-2})$	3.78×10^{-2}; $(3.19 \times 10^{-2}, 4.57 \times 10^{-2})$
Edge-effects, τ	0	0.54; (0.42, 0.66)*	0.43; (0.31, 0.54)*	0.50; (0.38, 0.62)*
Invasion suitability (due to environment)				
$\beta_{temperature}$	0	1.08; (1.02, 1.14)*	0.78; (0.74, 0.82)*	0.75; (0.71, 0.79)*
$\beta_{precipitation}$	0	0.38; (0.34, 0.42)*	0.28; (0.24, 0.31)*	0.27; (0.23, 0.30)*
$\beta_{cropland\ area}$	0	-0.00; (-0.06, 0.06)	0.03; (-0.02, 0.07)	0.01; (-0.03, 0.06)
$\beta_{urban\ area}$	0	0.18; (0.13, 0.22)*	0.15; (0.11, 0.18)*	0.14; (0.11, 0.18)*
$\beta_{motorways}$	0	0.03; (0.00, 0.06)*	0.01; (-0.01, 0.03)	0.01; (-0.01, 0.04)
$\beta_{railways}$	0	0.14; (0.10, 0.17)*	0.10; (0.06, 0.13)*	-0.03; (-0.08, 0.02)
Isotropic dispersal, α	$\rightarrow\infty$ (all $d_{j,i} \geq 1$)	1.11; (1.03, 1.19)	1.22; (1.14, 1.30)	1.43; (1.32, 1.54)
Source cells propagule production rate, η	0	3.18×10^{-2}; $(2.95 \times 10^{-2}, 3.42 \times 10^{-2})$	2.39×10^{-2}; $(2.15 \times 10^{-2}, 2.63 \times 10^{-2})$	2.22×10^{-2}; $(2.00 \times 10^{-2}, 2.46 \times 10^{-2})$
Invasion level dynamics (within-cell)				
Initial value, N_0	$N_0 = K_i = 1$		3.84×10^{0}; $(3.25 \times 10^{0}, 2.36 \times 10^{2})$	3.66×10^{0}; $(3.00 \times 10^{0}, 3.33 \times 10^{2})$
Intrinsic growth rate, r	0		4.10×10^{-4}; $(3.73 \times 10^{-5}, 1.61 \times 10^{-3})$	4.13×10^{-4}; $(3.83 \times 10^{-5}, 1.68 \times 10^{-3})$
Extrinsic growth rate, s	0		4.89×10^{-4}; $(4.35 \times 10^{-5}, 1.99 \times 10^{-3})$	4.26×10^{-4}; $(3.79 \times 10^{-5}, 1.74 \times 10^{-3})$
Anisotropic dispersal (along networks)				
ω_{roads}	0			1.53×10^{-3}; $(1.61 \times 10^{-4}, 4.93 \times 10^{-3})$
$\omega_{railways}$	0			5.89×10^{-2}; $(3.78 \times 10^{-2}, 8.36 \times 10^{-2})$

between models, pronounced divergences in parameter estimates were found. This was particularly noticeable between Model 1 and the other models, and for the most discriminative climate variables for which two pronounced shifts of parameter estimates occurred: the first when introducing invaded cells as propagule sources (Model 3), and the second when modelling within-cell invasion level dynamics of these source cells (Model 5) (Table 1).

Contrasting Model 1 vs. 2, both of which used only background introductions as the sole propagule source, the latter estimated a pronounced time trend with invasion risk rising sharply in recent decades (Figure 3a,b, Table 1). However, once invaded cells themselves were modelled to act as spread propagators (Models 3–6), their importance as propagule sources increased as the study area became progressively more invaded. Towards the end of the 20th century, their contribution to invasion risk dominated by about one order of magnitude

over background introductions (Figure 3c–f), resulting in autochthonous spread with exponential invasion acceleration.

For isotropic dispersal, the shape of the kernel function remained very similar across all models and suggested that most dispersal occurred within a distance of a few cells (Figure 4, Table 1).

The edge-effects term (Models 4–6) significantly improved the spread pattern explanation, but its importance was minor compared to source cells with an explicit lattice system representation (Tables 1 and 2).

For within-cell invasion level dynamics, the initial value was rather large but growth rates low (Table 1). While reliable bulk-up dynamics could hence not be estimated based on the occurrence data that we used, for many invaded cells, their maximum invasion level acted as the effective limiting factor (0.05 and 0.95 p-quantiles of these levels for invaded cells: Model 5: 0.8 and 3.7, respectively;
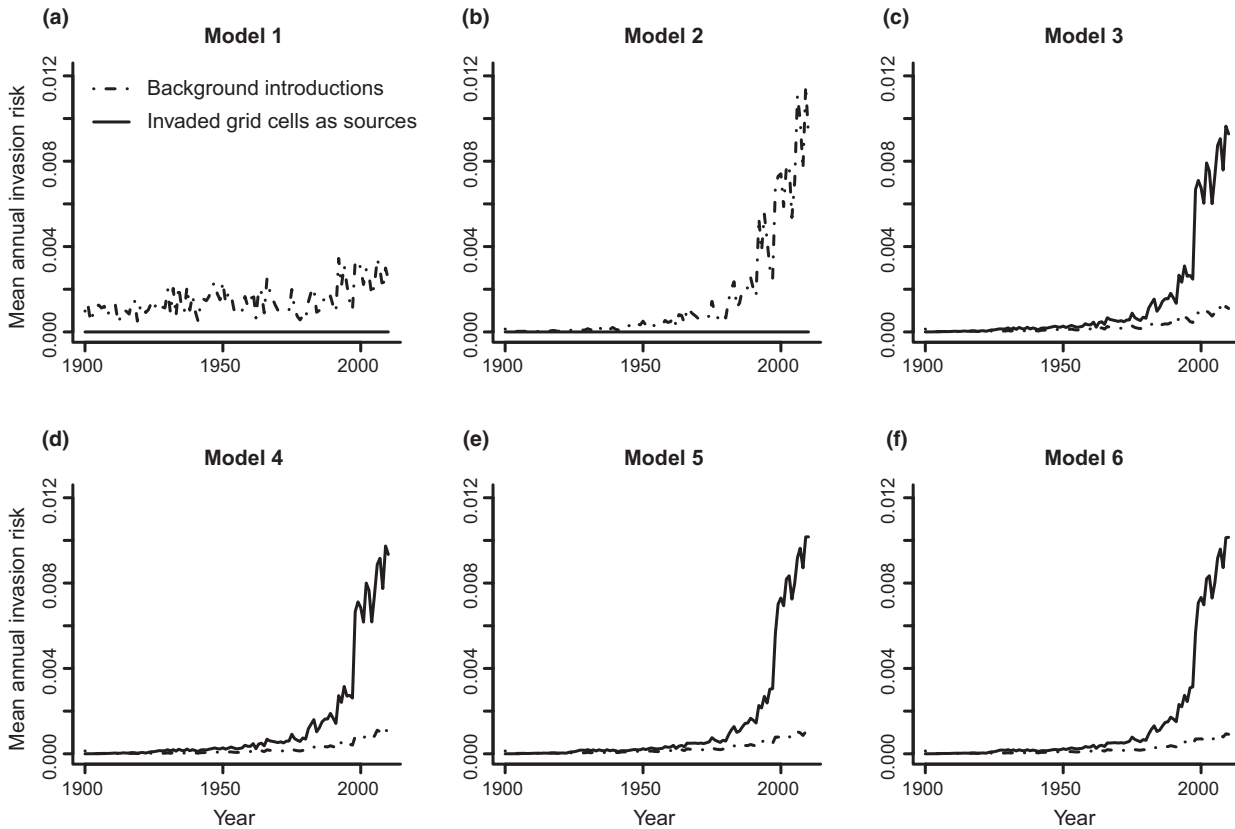
FIGURE 3 Average annual invasion risk values of uninvaded grid cells for six increasingly more complex models (a-f) of *Ambrosia artemisiifolia* invasion in Central Europe. The invasion risk is separated into the contributions of "background" introductions as a global, spatially implicit propagule source (used by all models, with a time trend for all but Model 1) and invaded cells acting as spread propagators (Models 3–6; Model 4 also introduces edge-effects, Model 5 spatio-temporal variability in source cell strength and Model 6 human-mediated dispersal along road and railway networks). Interannual variation is enhanced by environmental variability over time (particularly climate variability)

Model 6: 0.8 and 3.2, respectively; Figure S1). Consequently, source cells in environmentally well-suited areas exerted amplified propagule pressure as they had higher invasion levels than source cells outside these areas.

Integrating anisotropic dispersal along roads and railways yielded a significant model improvement (Tables 1 and 2). Contrasting the various dispersal means at the study scale and resolution, isotropic dispersal was overall the more influential spreading mechanism, but anisotropic dispersal gained in importance as distance increased.

Invasion risk was determined by environmental heterogeneity affecting invasion suitability; background introductions; source cells and their invasion level; and dispersal means from these foci. Consequently, Models 1 and 2, both of which did not account for invaded cells as spread propagators, yielded spatio-temporal invasion risk patterns that were substantially different from all subsequent models (Figure 5).

3.2 | Model hierarchy

When models were contrasted using DIC, the results showed that each more elaborate model was a significant improvement compared to its predecessors (Table 2). However, improvement was particularly pronounced for Models 1-3, which introduced differences in

invasion suitability dependent on environmental conditions, temporal variability in background introductions and source cells as spread propagators, respectively. Adding spatio-temporal variability in the propagule production of source cells by modelling within-cell invasion level dynamics (Model 5) also had a rather large impact. By contrast, the integration of edge-effects and anisotropic dispersal means resulted in only relatively minor improvements (Table 2).

The AUC improved substantially with each of the first three models but then remained almost identical at a rather high value of 0.93 for all subsequent models (Table 2). For Tjur's coefficient of discrimination, the individual fit improvement steps more closely resembled those of the DIC, but at a maximum value of 0.035 (Models 5 and 6), it was relatively low (Table 2). The more complex models thus had greater power to identify a relatively small subset of cells as likely candidates for the next invasion, but among these cells considerable uncertainty with respect to the specific invasion events remained.

4 | DISCUSSION

With the advance of computer power and numerical techniques, spatio-temporal spread models which integrate effects of the environment and population dynamics (Gallien, Münkemüller, Albert, Boulangeat, &

Thuiller, 2010; Marion et al., 2012; Pagel & Schurr, 2012) have seen recent proliferation. For the particular case of biological invasions, incorporating human-mediated dispersal may also be essential (Chapman et al., 2016; Drake & Mandrak, 2010). The framework we present here provides a flexible means of building and fitting such integrated models for analysing biological invasions. Specific models of individual invasion studies are created by selecting and combining modules that represent processes assumed to determine these invasions. We emphasize that for each module, many different implementations beyond our *A. artemisiifolia* case study application are possible.

4.1 | Integrated modelling

Our framework jointly integrates and fits parameters of several processes hypothesized to (co)determine any specific invasion. By contrast, hybrid models sequentially link several submodels of different
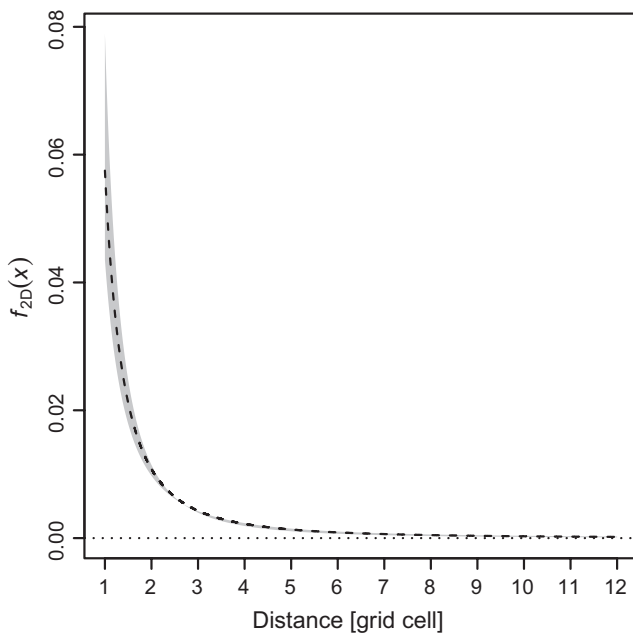
FIGURE 4 Kernel function for isotropic dispersal from source to recipient cells in the two-dimensional lattice system used in the models of *Ambrosia artemisiifolia* invasion in Central Europe. The dashed line shows the function for an intermediate value of the shape parameter ($\alpha = 1.24$), and the shaded area marks the function's range between $\alpha = 1.03$ and $\alpha = 1.54$, the minimum and maximum value, respectively, of any model's 95% credible interval for α (cf. Table 1)

kinds (Gallien et al., 2010; Smolik et al., 2010), for example by first fitting a species distribution model and subsequently using its output to parameterize a spatially explicit spread model. The integrated approach has the advantage that biases are reduced as model fitting accounts for the combined effects of all investigated processes (Pagel & Schurr, 2012). Moreover, it avoids circularity problems (Gallien et al., 2010) and assumptions about scaling relationships among the ecological processes represented by the different submodels in hybrid modelling (Thuiller et al., 2014). The case of *A. artemisiifolia* demonstrates how jointly fitting different drivers may affect quantitative and even qualitative inferences about the role of any individual driver: both the overall importance of environmental conditions on the spatio-temporal spread dynamics and the particular impact of individual environmental variables changed profoundly along our model hierarchy. Model 6 even entirely shifted the role of motorways and railways from a determinant of environmental suitability for invasion to a dispersal means. However, jointly fitting all processes of interest typically requires that own parameter estimation routines with potentially high computing costs must be provided. Consequently, in our case study, we used a rather simplistic linear combination of environmental variables and free parameters, similar to a generalized linear model (GLM; Faraway, 2006), to model the dependence of local invasion suitability on environmental conditions. As such, this approach does not exploit the power of more advanced algorithms that are commonly applied in purely correlative niche models (Elith et al., 2006). We argue, however, that in our process-based modelling framework (Dormann et al., 2012), the potentially reduced fit for single individual invasion drivers is more than compensated for by more realistic inferences about the relative roles of the modelled drivers and their interplay. Additionally, the modular design of our framework encourages the use of customized formulae (such as specifically accounting for species' life-history traits) to numerically represent the modelled invasion processes. Furthermore, these individual processes can potentially be associated with stochasticity and models fitted by means of hierarchical modelling (Marion et al., 2012; Wikle, 2003) or likelihood approximation methods (Hartig, Calabrese, Reineking, Wiegand, & Huth, 2011; Rasmussen & Hamilton, 2012).

4.2 | Framework applications

Our framework uses a statistical approach and fits models using spatio-temporal distribution data from the invading species in the
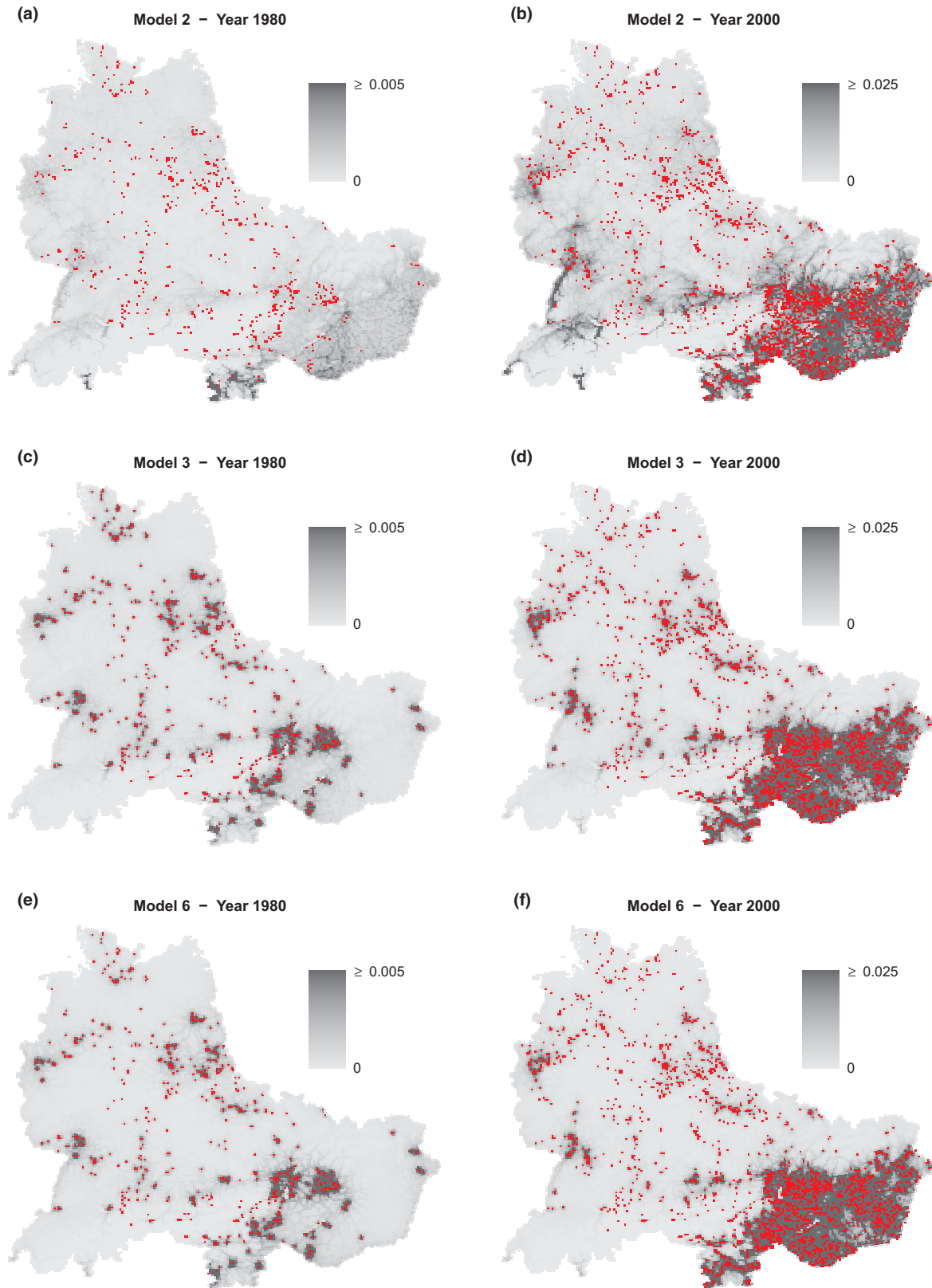
TABLE 2 Fit statistics for all models. In ascending order, each model integrates additional processes assumed to determine the invasion of *Ambrosia artemisiifolia* in Central Europe (cf. Table 1). DIC: Deviance Information Criterion; AUC: area under the receiver operating characteristic curve

Statistic	Null-model	Model 1	Model 2	Model 3	Model 4	Model 5	Model 6
DIC	53966.0	47147.8	42541.5	39337.1	39265.7	38865.6	38829.2
ΔDIC (from preceding model)		−6818.2	−4606.3	−3204.4	−71.4	−400.1	−36.4
AUC	0.658	0.846	0.904	0.929	0.930	0.930	0.931
Tjur's coefficient of discrimination	0.000	0.006	0.016	0.030	0.030	0.035	0.035

FIGURE 5 Annual invasion probabilities of grid cells (conditional on cells not having been invaded by the preceding year) estimated by three models for both a year before (1980) and during (2000) the rapid spreading phase of *Ambrosia artemisiifolia* in Central Europe (cf. Figures 2 and 3). Cells already invaded are shown in red. Model 2 (a,b) assumes that the invasion pattern is driven by environmental heterogeneity but independent of already invaded cells. Model 3 (c,d) and Model 6 (e,f) additionally account for the spread from invaded to uninvaded cells, with the latter model further integrating edge-effects, spatio-temporal variability in the propagule production of source cells and anisotropic dispersal along road and railway networks. [Colour figure can be viewed at wileyonlinelibrary.com]

study area (Cook et al., 2007; Marion et al., 2012). A central aim here is to test hypotheses about the unknown effects of specific drivers on observed invasion patterns. For this purpose, the particular drivers are implemented as relatively generic functional structures for which the specific shape is then determined by parameter estimation to infer their contributions to spread rates at the grid cell scale. By contrast, models simulating the development of individuals or populations (Fitzpatrick et al., 2012; Sebert-Cuvillier et al., 2010) and phenology models (Chapman et al., 2014) scale more directly to real-world properties, such as species' demographic rates, dispersal distances of individual propagules or physiological constraints. However, parameterizing these models may require considerable a priori knowledge of the modelled invasion processes, both in terms of their functional forms and specific parameter values. Where such expert knowledge is (partly) available and scalable to grid cells, in our framework, it can also be used to specify individual modules with greater detail or to provide informative prior distributions. For example, if resident species are known to influence biotic resistance to invasion (Levine, Adler, & Yelenik, 2004), spatially explicit information on these species could be used to adjust both invasion risk of uninvaded cells and maximum invasion levels within colonized cells.

Although our framework focuses on analysing and understanding observed invasions, once a model is parameterized and considered to be robust, it can also be used to predict the likely future spread of the species by means of forward simulation. These projections could guide specific risk assessments, such as the likelihood of spread into nature conservation areas, or be used to estimate when the total number of grid cells invaded will exceed a predefined critical threshold. As an additional application, the effectiveness of proposed management strategies could be explored by simulating future spread under various control measures such as reduction in population density in invaded cells, local eradication or containment by preventing dispersal between cells (Richter et al., 2013; Walker, Poos, & Groeneveld, 2015). In these simulations, the economically best strategy could be identified by relating the costs of surveillance and control efforts to the decrease in invasion density and hence reduction in damage caused by the invading species (Epanchin-Niell & Hastings, 2010). As our framework is spatio-temporally explicit, the effects of allocating control resources heterogeneously over space and time, for example dependent on the distribution pattern of species abundance or habitat fragmentation (Baker, 2017; Meier et al., 2014), could also be tested. Moreover, the quantitative inferences on invasion drivers obtained from our framework could be used for more accurately parameterizing bioeconomic models which take account of multiple constraints in seeking the optimal control policy (Epanchin-Niell & Hastings, 2010).

4.3 | Model choices and assumptions

Choosing practical models involves ensuring that important invasion determinants are integrated, while avoiding overly complex models.

In Models 5 and 6, we reused the invasion suitability module first introduced in Model 1 as an efficient means of representing differences in the strength of source cells, and therefore differences in average population sizes of *A. artemisiifolia* in the study area, subject to local environmental conditions. This module reuse avoids the need for estimating additional parameters, but, as a trade-off, implies that the individual environmental variables are assumed to affect invasion risk of recipient cells and maximum strength of source cells in the same manner. Similarly, the module representing within-cell invasion level dynamics could be extended to account for differences in propagule influx into cells by modelling the initial invasion level and extrinsic growth rate as dependent on the particular invasion state of surrounding cells. This approach would considerably increase computational costs but may be particularly worthwhile if data also document abundance changes within cells. For our case study, however, we only had occurrence data at our disposal and hence could not model within-cell invasion level dynamics realistically.

Our framework does not consider detection errors and biases in the species dataset. In practice, however, species records may lag behind actual first colonizations of grid cells and not all cells actually invaded may be documented. In this case, a systematic underestimation of cell colonization rates must be anticipated where expert knowledge may guide the estimation of the error magnitude. To yield robust inferences about individual invasion processes, the study period should be much larger than average detection time-lags, and a sufficiently large distribution dataset should be available for the study grid. Moreover, spatio-temporal differences in data quality should be unrelated to characteristic invasion patterns themselves, for example sampling intensity should not vary with climatic region. For a statistical approach that explicitly accounts for imperfect spread observation, see Mang et al. (2017).

5 | CONCLUSIONS

The framework presented here provides a flexible means for integrated, spatio-temporal modelling of biological invasions. The process-based models (Dormann et al., 2012) derived from it and the statistical implementation allow the testing of hypotheses about the impact of suggested key invasion determinants. Additionally, the framework's generic, modular design facilitates its application to different observed invasions. In our case study application, all modelled processes were shown to have a significant effect. Nevertheless, in terms of balancing fit quality with model complexity, the most substantial improvements were achieved up to Model 3 which introduced basic source-recipient cell relationships and also by modelling differences in source strength among invaded cells (introduced in Model 5). We therefore conclude that for efficient invasion modelling, it is important to represent changes in spatio-temporal propagule supply by explicitly tracking the colonization sequence and establishment of new populations. More elaborate models may explore in greater detail the specific roles and functional forms of processes involved in species spread.

ORCID

Thomas Mang iD http://orcid.org/0000-0001-5206-2981

REFERENCES

Andrew, M. E., & Ustin, S. L. (2010). The effects of temporally variable dispersal and landscape structure on invasive species spread. *Ecological Applications*, *20*, 593–608. https://doi.org/10.1890/09-0034.1

Baker, C. M. (2017). Target the source: Optimal spatiotemporal resource allocation for invasive species control. *Conservation Letters*, *10*, 41–48. https://doi.org/10.1111/conl.12236

Bellard, C., Cassey, P., & Blackburn, T. M. (2016). Alien species as a driver of recent extinctions. *Biology Letters*, *12*, 1–4. https://doi.org/10.1098/rsbl.2015.0623

Chapman, D. S., Haynes, T., Beal, S., Essl, F., & Bullock, J. M. (2014). Phenology predicts the native and invasive range limits of common ragweed. *Global Change Biology*, *20*, 192–202. https://doi.org/10.1111/gcb.12380

Chapman, D. S., Makra, L., Albertini, R., Bonini, M., Páldy, A., Rodinkova, V., ... Bullock, J. M. (2016). Modelling the introduction and spread of non-native species: International trade and climate change drive ragweed invasion. *Global Change Biology*, *22*, 3067–3079. https://doi.org/10.1111/gcb.13220

Cook, A., Marion, G., Butler, A., & Gibson, G. (2007). Bayesian inference for the spatio-temporal invasion of alien species. *Bulletin of Mathematical Biology*, *69*, 2005–2025. https://doi.org/10.1007/s11538-007-9202-4

DiTommaso, A. (2004). Germination behavior of common ragweed (*Ambrosia artemisiifolia*) populations across a range of salinities. *Weed Science*, *52*, 1002–1009. https://doi.org/10.1614/WS-04-030R1

Dormann, C. F., Schymanski, S. J., Cabral, J., Chuine, I., Graham, C., Hartig, F., ... Singer, A. (2012). Correlation and process in species distribution models: Bridging a dichotomy. *Journal of Biogeography*, *39*, 2119–2131. https://doi.org/10.1111/j.1365-2699.2011.02659.x

Drake, D. A. R., & Mandrak, N. E. (2010). Least-cost transportation networks predict spatial interaction of invasion vectors. *Ecological Applications*, *20*, 2286–2299. https://doi.org/10.1890/09-2005.1

Dullinger, S., Kleinbauer, I., Peterseil, J., Smolik, M., & Essl, F. (2009). Niche based distribution modelling of an invasive alien plant: Effects of population status, propagule pressure and invasion history. *Biological Invasions*, *11*, 2401–2414. https://doi.org/10.1007/s10530-009-9424-5

Elith, J., Graham, C. H., Anderson, R. P., Dudík, M., Ferrier, S., Guisan, A., ... Zimmermann, N. E. (2006). Novel methods improve prediction of species' distributions from occurrence data. *Ecography*, *29*, 129–151. https://doi.org/10.1111/j.2006.0906-7590.04596.x

Elith, J., Kearney, M., & Phillips, S. (2010). The art of modelling range-shifting species. *Methods in Ecology and Evolution*, *1*, 330–342. https://doi.org/10.1111/j.2041-210X.2010.00036.x

Epanchin-Niell, R. S., & Hastings, A. (2010). Controlling established invaders: Integrating economics and spread dynamics to determine optimal management. *Ecology Letters*, *13*, 528–541. https://doi.org/10.1111/j.1461-0248.2010.01440.x

Essl, F., Biró, K., Brandes, D., Broennimann, O., Bullock, J. M., Chapman, D. S., ... Follak, S. (2015). Biological Flora of the British Isles: *Ambrosia artemisiifolia*. *Journal of Ecology*, *103*, 1069–1098. https://doi.org/10.1111/1365-2745.12424

Faraway, J. J. (2006). *Extending the linear model with R: Generalized linear, mixed effects and nonparametric regression models*. Boca Raton, FL: Chapman & Hall/CRC.

Fitzpatrick, M. C., Preisser, E. L., Porter, A., Elkinton, J., & Ellison, A. M. (2012). Modeling range dynamics in heterogeneous landscapes: Invasion of the hemlock woolly adelgid in eastern North America. *Ecological Applications*, *22*, 472–486. https://doi.org/10.1890/11-0009.1

Gallien, L., Münkemüller, T., Albert, C. H., Boulangeat, I., & Thuiller, W. (2010). Predicting potential distributions of invasive species: Where to go from here? *Diversity and Distributions*, *16*, 331–342. https://doi.org/10.1111/j.1472-4642.2010.00652.x

Gelman, A., Carlin, J. B., Stern, H. S., & Rubin, D. B. (2004). *Bayesian data analysis*, 2nd ed. Boca Raton, FL: Chapman and Hall/CRC.

Hartig, F., Calabrese, J. M., Reineking, B., Wiegand, T., & Huth, A. (2011). Statistical inference for stochastic simulation models – theory and application. *Ecology Letters*, *14*, 816–827. https://doi.org/10.1111/j.1461-0248.2011.01640.x

Hastings, A., Cuddington, K., Davies, K. F., Dugaw, C. J., Elmendorf, S., Freestone, A., ... Thomson, D. (2005). The spatial spread of invasions: New developments in theory and evidence. *Ecology Letters*, *8*, 91–101. https://doi.org/10.1111/j.1461-0248.2004.00687.x

Jongejans, E., Shea, K., Skarpaas, O., Kelly, D., & Ellner, S. P. (2011). Importance of individual and environmental variation for invasive species spread: A spatial integral projection model. *Ecology*, *92*, 86–97. https://doi.org/10.1890/09-2226.1

Kadoya, T., & Washitani, I. (2010). Predicting the rate of range expansion of an invasive alien bumblebee (*Bombus terrestris*) using a stochastic spatio-temporal model. *Biological Conservation*, *143*, 1228–1235. https://doi.org/10.1016/j.biocon.2010.02.030

Kot, M., Lewis, M. A., & van den Driessche, P. (1996). Dispersal data and the spread of invading organisms. *Ecology*, *77*, 2027–2042. https://doi.org/10.2307/2265698

Levine, J. M., Adler, P. B., & Yelenik, S. G. (2004). A meta-analysis of biotic resistance to exotic plant invasions. *Ecology Letters*, *7*, 975–989. https://doi.org/10.1111/j.1461-0248.2004.00657.x

Mack, R. N., Simberloff, D., Lonsdale, W. M., Evans, H., Clout, M., & Bazzaz, F. A. (2000). Biotic invasions: Causes, epidemiology, global consequences, and control. *Ecological Applications*, *10*, 689–710. https://doi.org/10.1890/1051-0761(2000)010[0689:BICEGC]2.0.CO;2

Mang, T., Essl, F., Moser, D., Karrer, G., Kleinbauer, I., & Dullinger, S. (2017). Accounting for imperfect observation and estimating true species distributions in modelling biological invasions. *Ecography*, *40*, 1187–1197. https://doi.org/10.1111/ecog.02194

Marion, G., McInerny, G. J., Pagel, J., Catterall, S., Cook, A. R., Hartig, F., & O'Hara, R. B. (2012). Parameter and uncertainty estimation for process-oriented population and distribution models: Data, statistics and the niche. *Journal of Biogeography*, *39*, 2225–2239. https://doi.org/10.1111/j.1365-2699.2012.02772.x

Medlock, J. M., Hansford, K. M., Schaffner, F., Versteirt, V., Hendrickx, G., Zeller, H., & Van Bortel, W. (2012). A review of the invasive mosquitoes in Europe: Ecology, public health risks, and control options. *Vector-Borne and Zoonotic Diseases*, *12*, 435–447. https://doi.org/10.1089/vbz.2011.0814

Meier, E. S., Dullinger, S., Zimmermann, N. E., Baumgartner, D., Gattringer, A., & Hülber, K. (2014). Space matters when defining effective management for invasive plants. *Diversity and Distributions*, *20*, 1029–1043. https://doi.org/10.1111/ddi.12201

Merow, C., LaFleur, N., Silander Jr, J. A., Wilson, A. M., & Rubega, M. (2011). Developing dynamic mechanistic species distribution models: Predicting bird-mediated spread of invasive plants across northeastern North America. *American Naturalist*, *178*, 30–43. https://doi.org/10.1086/660295

Muirhead, J. R., Leung, B., van Overdijk, C., Kelly, D. W., Nandakumar, K., Marchant, K. R., & MacIsaac, H. J. (2006). Modelling local and long-distance dispersal of invasive emerald ash borer *Agrilus planipennis* (Coleoptera) in North America. *Diversity and Distributions*, *12*, 71–79. https://doi.org/10.1111/j.1366-9516.2006.00218.x

Neubert, M. G., & Parker, I. M. (2004). Projecting rates of spread for invasive species. *Risk Analysis*, *24*, 817–831. https://doi.org/10.1111/j.0272-4332.2004.00481.x

Pagel, J., & Schurr, F. M. (2012). Forecasting species ranges by statistical estimation of ecological niches and spatial population dynamics. *Global Ecology and Biogeography*, *21*, 293–304. https://doi.org/10.1111/j.1466-8238.2011.00663.x

Pauchard, A., & Shea, K. (2006). Integrating the study of non-native plant invasions across spatial scales. *Biological Invasions*, *8*, 399–413. https://doi.org/10.1007/s10530-005-6419-8

Pejchar, L., & Mooney, H. A. (2009). Invasive species, ecosystem services and human well-being. *Trends in Ecology & Evolution*, *24*, 497–504. https://doi.org/10.1016/j.tree.2009.03.016

Peterson, A. T. (2003). Predicting the geography of species' invasions via ecological niche modeling. *Quarterly Review of Biology*, *78*, 419–433. https://doi.org/10.1086/378926

Petitpierre, B., Kueffer, C., Broennimann, O., Randin, C., Daehler, C., & Guisan, A. (2012). Climatic niche shifts are rare among terrestrial plant invaders. *Science*, *335*, 1344–1348. https://doi.org/10.1126/science.1215933

Pimentel, D., Zuniga, R., & Morrison, D. (2005). Update on the environmental and economic costs associated with alien-invasive species in the United States. *Ecological Economics*, *52*, 273–288. https://doi.org/10.1016/j.ecolecon.2004.10.002

Portnoy, S., & Willson, M. F. (1993). Seed dispersal curves: Behavior of the tail of the distribution. *Evolutionary Ecology*, *7*, 25–44. https://doi.org/10.1007/BF01237733

Potapov, A., Muirhead, J. R., Lelea, S. R., & Lewis, M. A. (2011). Stochastic gravity models for modeling lake invasions. *Ecological Modelling*, *222*, 964–972. https://doi.org/10.1016/j.ecolmodel.2010.07.024

Pyšek, P., & Richardson, D. M. (2007). Traits associated with invasiveness in alien plants: Where do we stand? In W. Nentwig (Ed.), *Biological invasions* (Vol. *193*, pp. 97–125). Berlin & Heidelberg: Springer.

Pyšek, P., & Richardson, D. M. (2010). Invasive species, environmental change and management, and health. In A. Gadgil & D. M. Liverman (Eds.), *Annual review of environment and resources* (Vol. *35*, pp. 25–55). Palo Alto, CA: Annual Reviews.

Rasmussen, R., & Hamilton, G. (2012). An approximate Bayesian computation approach for estimating parameters of complex environmental processes in a cellular automata. *Environmental Modelling & Software*, *29*, 1–10. https://doi.org/10.1016/j.envsoft.2011.10.005

Richter, R., Berger, U. E., Dullinger, S., Essl, F., Leitner, M., Smith, M., & Vogl, G. (2013). Spread of invasive ragweed: Climate change, management and how to reduce allergy costs. *Journal of Applied Ecology*, *50*, 1422–1430. https://doi.org/10.1111/1365-2664.12156

Sakai, A. K., Allendorf, F. W., Holt, J. S., Lodge, D. M., Molofsky, J., With, K. A., ... Weller, S. G. (2001). The population biology of invasive species. *Annual Review of Ecology and Systematics*, *32*, 305–332. https://doi.org/10.1146/annurev.ecolsys.32.081501.114037

Sebert-Cuvillier, E., Simonet, M., Simon-Goyheneche, V., Paccaut, F., Goubet, O., & Decocq, G. (2010). *PRUNUS*: A spatially explicit demographic model to study plant invasions in stochastic, heterogeneous environments. *Biological Invasions*, *12*, 1183–1206. https://doi.org/10.1007/s10530-009-9539-8

Smolik, M. G., Dullinger, S., Essl, F., Kleinbauer, I., Leitner, M., Peterseil, J., ... Vogl, G. (2010). Integrating species distribution models and interacting particle systems to predict the spread of an invasive alien plant. *Journal of Biogeography*, *37*, 411–422. https://doi.org/10.1111/j.1365-2699.2009.02227.x

Spiegelhalter, D. J., Best, N. G., Carlin, B. P., & van der Linde, A. (2002). Bayesian measures of model complexity and fit. *Journal of the Royal Statistical Society: Series B (Statistical Methodology)*, *64*, 583–639. https://doi.org/10.1111/1467-9868.00353

Strayer, D. L., Eviner, V. T., Jeschke, J. M., & Pace, M. L. (2006). Understanding the long-term effects of species invasions. *Trends in Ecology & Evolution*, *21*, 645–651. https://doi.org/10.1016/j.tree.2006.07.007

Taramarcaz, P., Lambelet, C., Clot, B., Keimer, C., & Hauser, C. (2005). Ragweed (Ambrosia) progression and its health risks: Will Switzerland resist this invasion? *Swiss Medical Weekly*, *135*, 538–548.

Thuiller, W., Münkemüller, T., Schiffers, K. H., Georges, D., Dullinger, S., Eckhart, V. M., ... Schurr, F. M. (2014). Does probability of occurrence relate to population dynamics? *Ecography*, *37*, 1155–1166. https://doi.org/10.1111/ecog.00836

Tjur, T. (2009). Coefficients of determination in logistic regression models—a new proposal: The coefficient of discrimination. *American Statistician*, *63*, 366–372. https://doi.org/10.1198/tast.2009.08210

Tsoularis, A., & Wallace, J. (2002). Analysis of logistic growth models. *Mathematical Biosciences*, *179*, 21–55. https://doi.org/10.1016/S0025-5564(02)00096-2

Vitousek, P. M., D'Antonio, C. M., Loope, L. L., & Westbrooks, R. (1996). Biological invasions as global environmental change. *American Scientist*, *84*, 468–478.

Walker, A. N., Poos, J.-J., & Groeneveld, R. A. (2015). Invasive species control in a one-dimensional metapopulation network. *Ecological Modelling*, *316*, 176–184. https://doi.org/10.1016/j.ecolmodel.2015.08.015

Wikle, C. K. (2003). Hierarchical Bayesian models for predicting the spread of ecological processes. *Ecology*, *84*, 1382–1394. https://doi.org/10.1890/0012-9658(2003)084[1382:HBMFPT]2.0.CO;2

BIOSKETCH

T.M.'s research focuses on the modelling of biodiversity patterns from local scales up to the global level, with a particular interest in non-native species and the determinants of their spread dynamics and invasion success.

Author contributions: T.M. and S.D. conceived the ideas; F.E., D.M. and I.K. collected the data; T.M. conducted the modelling and analyses; T.M. and S.D. led the writing, and F.E. and D.M. contributed to the writing.

SUPPORTING INFORMATION

Additional Supporting Information may be found online in the supporting information tab for this article.